LOAN DOCUMENT

PHOTOGRAPH THIS SHEET

AD-A239 096

DTIC ACCESSION NUMBER

LEVEL

INVENTORY 1

The Bandwidth Performance of a Two-Element ... etc.

DOCUMENT IDENTIFICATION

Apr 1986

DISTRIBUTION STATEMENT

ACCESSION FOR

NTIS GRA&I ☑

DTIC TRAC ☐

UNANNOUNCED ☐

JUSTIFICATION

BY Per AD34 095

DISTRIBUTION/

AVAILABILITY CODES

DISTRIBUTION	AVAILABILITY AND/OR SPECIAL	
A-1		

DISTRIBUTION STAMP

DTIC

DATE ACCESSIONED

DATE RETURNED

91 7 30 023

23 91-06530

DATE RECEIVED IN DTIC

REGISTERED OR CERTIFIED NUMBER

PHOTOGRAPH THIS SHEET AND RETURN TO DTIC-FDAC

DTIC FORM 70A JUN 90

DOCUMENT PROCESSING SHEET

PREVIOUS EDITIONS MAY BE USED UNTIL STOCK IS EXHAUSTED

LOAN DOCUMENT

HANDLE WITH CARE

The Ohio State University

THE BANDWIDTH PERFORMANCE OF A TWO-ELEMENT ADAPTIVE ARRAY WITH TAPPED DELAY-LINE PROCESSING

R.T. Compton, Jr.

The Ohio State University

ElectroScience Laboratory

Department of Electrical Engineering
Columbus, Ohio 43212

Quarterly Technical Report 717253-3
Contract N00019-85-C-0119
April 1986

Department of the Navy
Naval Air Systems Command
Washington, DC 20361

NOTICES

When Government drawings, specifications, or other data are used for any purpose other than in connection with a definitely related Government procurement operation, the United States Government thereby incurs no responsibility nor any obligation whatsoever, and the fact that the Government may have formulated, furnished, or in any way supplied the said drawings, specifications, or other data, is not to be regarded by implication or otherwise as in any manner licensing the holder or any other person or corporation, or conveying any rights or permission to manufacture, use, or sell any patented invention that may in any way be related thereto.

50272-101

REPORT DOCUMENTATION PAGE	1. REPORT NO. 717253-3	2.	3. Recipient's Accession No.
4. Title and Subtitle: The Bandwidth Performance of a Two-Element Adaptive Array with Tapped Delay-Line Processing			5. Report Date: April 1986 6.
7. Author(s): R.T. Compton, Jr.			8. Performing Organization Rept. No. 717253-3
9. Performing Organization Name and Address: The ElectroScience Laboratory The Ohio State University 1320 Kinnear Road Columbus, Ohio 43212			10. Project/Task/Work Unit No. 11. Contract(C) or Grant(G) No (C) N00019-85-C-0119 (G)
12. Sponsoring Organization Name and Address: Department of the Navy Naval Air Systems Command Washington, DC 20361			13. Type of Report & Period Covered: Quarterly Technical 14.

15. Supplementary Notes

16. Abstract (Limit: 200 words)

We examine the bandwidth performance of a two-element adaptive array with a tapped delay-line behind each element. We show how the number of taps and the delay between taps affect the bandwidth performance of the array.

We show that an array with two weights and one delay behind each element yields optimal performance (equal to that obtained with CW interference) for any value of delay greater than zero and less than T_{90}/B, where T_{90} is the time delay for a 90° carrier phase shift and B is the fractional signal bandwidth. Delays less than T_{90} yield optimal performance but result in large array weights. Delays larger than T_{90}/B yield suboptimal SINR when each element has only two weights.

For delays between T_{90}/B and $4T_{90}/B$, the performance is suboptimal with only two taps but approaches the optimal if more taps are added to each element. Delays larger than $4T_{90}/B$ result in suboptimal performance regardless of the number of taps used.

17. Document Analysis a. Descriptors

b. Identifiers/Open-Ended Terms

c. COSATI Field/Group

18. Availability Statement	19. Security Class (This Report)	21. No of Pages
A. Approved for public release; distribution is unlimited.	Unclassified	40
	20. Security Class (This Page): Unclassified	22. Price

(See ANSI-Z39.18) See Instructions on Reverse OPTIONAL FORM 272 (4-77) (Formerly NTIS-35) Department of Commerce

TABLE OF CONTENTS

LIST OF FIGURES

I. INTRODUCTION

It is well known that the ability of an adaptive array to null interference deteriorates rapidly as the interference bandwidth increases [1-4]. However, using tapped delay-lines behind the elements improves the bandwidth performance. The purpose of this report is to examine how the improvement depends on the number of taps and the amount of delay between taps for a simple two-element array.

The use of tapped delay lines in an adaptive array was first suggested by Widrow et al [1] and has since been studied by several others. In one study, Rodgers and Compton [2] compared the performance of a two-element array with 2-, 3- and 5-tap delay lines and real weights to that of an array using a single complex weight behind each element. In another work, Mayhan, Simmons and Cummings [3] presented an analysis of how the number of elements and the number of delay line taps affect the interference cancellation ratio as a function of bandwidth. In addition, White [4] has studied the tradeoff between the number of interfering signals and the required number of auxiliary elements and delay line taps in an Applebaum array.

In Section II of this report, we formulate the equations needed to calculate the output SINR (signal-to-interference-plus-noise ratio) from an array with M elements and K delay line taps behind each element. Then, in Section III, we use these equations to determine the bandwidth performance of a two-element array. We show how the performance depends on the number of taps behind each element and the amount of delay between taps.

The results in this report have been obtained as part of a larger study, whose purpose is to relate the bandwidth performance of arrays using tapped delay-lines to that of arrays using FFTs (Fast Fourier Transforms) behind the elements. In this report, we discuss only arrays with tapped delay-line processing. The use of FFT processing will be taken up in a later report.

II. FORMULATION OF THE PROBLEM

Consider an adaptive array with M elements, as shown in Figure 1. Let the elements be isotropic and uniformly spaced along a line every half wavelength at the signal carrier frequency ω_o. Assume each element in Figure 1 is followed by a tapped delay-line with K taps and a delay of T_o seconds between taps. The output of the first tap behind each element is the element signal itself, with no delay. Let $\tilde{x}_{mk}(t)$ denote the (analytic) signal from element m at tap k. Thus, $\tilde{x}_{11}(t)$ is the signal received on element 1, $\tilde{x}_{21}(t)$ is the signal on element 2, $\tilde{x}_{12}(t)=\tilde{x}_{11}(t-T_o)$, $\tilde{x}_{1k}(t)=\tilde{x}_{11}(t-[K-1]T_o)$, and so forth.

We assume the tap signals are combined with an adaptive processor. This processor multiplies each $\tilde{x}_{mk}(t)$ by a complex weight w_{mk} and then sums the signals to produce the array output $\tilde{s}(t)$, as shown in Figure 1. The adaptive processor could consist of a set of analog LMS or Applebaum loops [1,5], or it could be a digital controller based on the Sample Matrix Inverse Method [6] or some other algorithm. All such processors attempt to adjust the array weights to their optimal values, which are known variously as the Wiener weights, the LMS (least mean square) weights, the Applebaum weights, or the maximum SINR (signal-to-

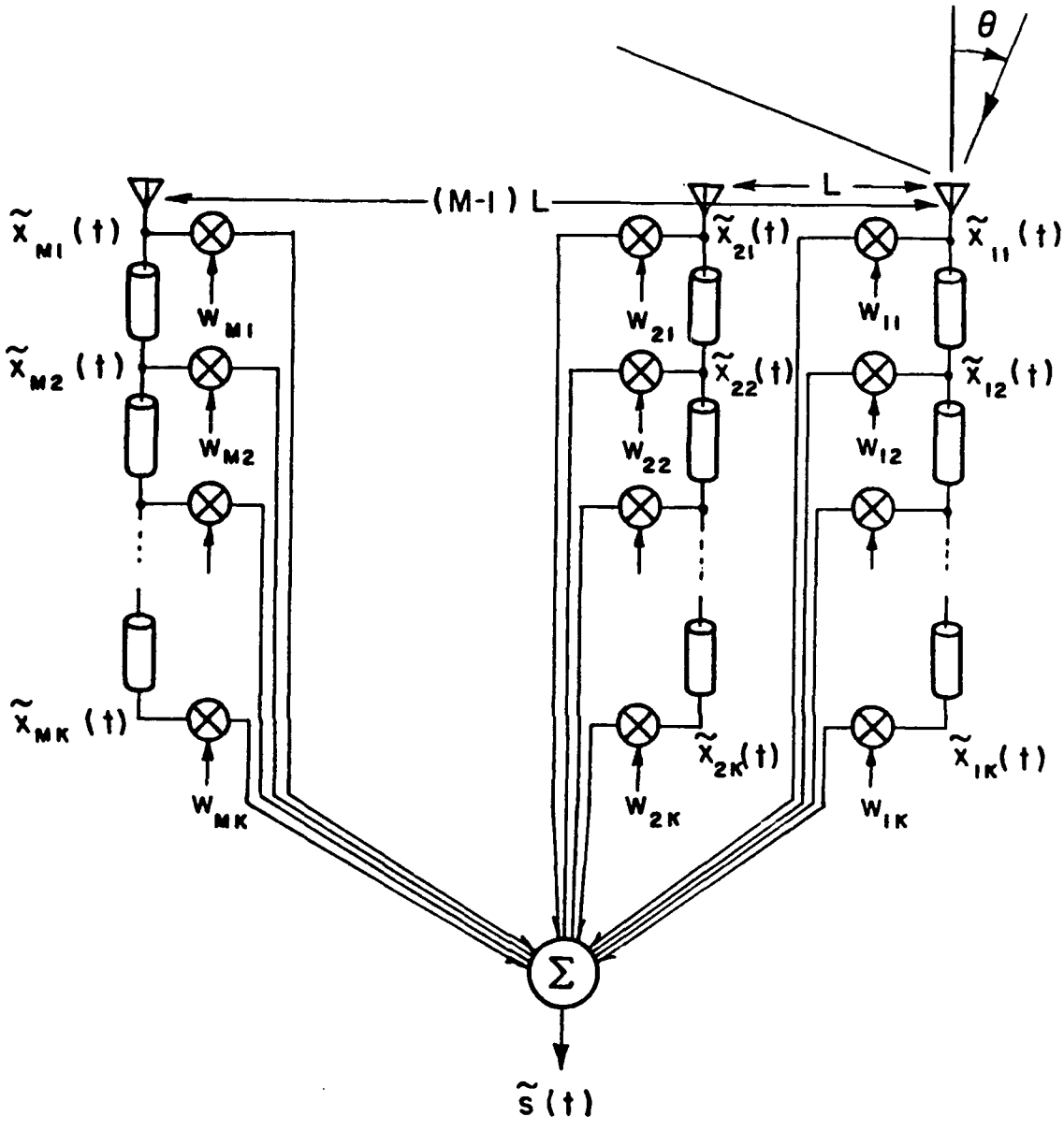

Figure 1. A Tapped Delay Line Adaptive Array.

interference-plus-noise ratio) weights. In this report, we shall not be concerned with the specific form of the adaptive processor, but shall simply assume that this processor adjusts the weights to their optimal values for any given set of incident signals.

For a given set of tap signals $\tilde{x}_{mk}(t)$, the optimal weights are found as follows. Let X_m and W_m (for $1 \leq m \leq M$) be column vectors containing the signals and weights at the K taps behind element m, i.e.

$$X_m = [\tilde{x}_{m1}(t), \tilde{x}_{m2}(t), \ldots, \tilde{x}_{mK}(t)]^T, \tag{1}$$

and

$$W_m = [w_{m1}, w_{m2}, \ldots, w_{mK}]^T. \tag{2}$$

(T denotes transpose.) We shall refer to X_m as the element signal vector and to W_m as the element weight vector. Then let X and W be the total signal and weight vectors for the entire array,

$$X = \begin{bmatrix} X_1 \\ X_2 \\ \cdot \\ \cdot \\ \cdot \\ X_M \end{bmatrix}, \tag{3}$$

and

$$W = \begin{bmatrix} W_1 \\ W_2 \\ \cdot \\ \cdot \\ \cdot \\ W_M \end{bmatrix}, \tag{4}$$

where we use a partitioned vector notation. The optimal weight vector in the array is then given by [1,5]

$$W = \Phi^{-1}S \ , \tag{5}$$

where Φ is the signal covariance matrix,

$$\Phi = E[X^{*}X^{T}] \ , \tag{6}$$

and S is the steering vector (or reference correlation vector),

$$S = E[X^{*}\tilde{d}_{0}(t)] \ . \tag{7}$$

In these equations, * denotes complex conjugate and $\tilde{d}_0(t)$ is a normalized replica of the desired signal to be received by the array. ($\tilde{d}_0(t)$ is defined below in (14).) The weight vector W satisfying (5) yields maximum SINR at the array output [1,5,7].

The $\tilde{x}_{mk}(t)$ may be determined from the signals incident on the array. For this study, we shall assume the array receives a desired signal and an interference signal, and that each element signal also contains an independent thermal noise voltage, as would be contributed by a front-end preamplifier or mixer. Thus, the signal at tap k behind element m has the form

$$\tilde{x}_{mk}(t) = \tilde{d}_{mk}(t) + \tilde{i}_{mk}(t) + \tilde{n}_{mk}(t) \ , \tag{8}$$

where $\tilde{d}_{mk}(t)$, $\tilde{i}_{mk}(t)$ and $\tilde{n}_{mk}(t)$ are the desired, interference and thermal noise components, respectively. The element signal vectors X_m and the total signal vector X may then be split in a similar way,

$$X_m = X_{dm} + X_{im} + X_{nm} \ , \tag{9}$$

and

$$X = X_d + X_i + X_n \ . \tag{10}$$

$\tilde{d}_{mk}(t)$, $\tilde{i}_{mk}(t)$ and $\tilde{n}_{mk}(t)$ may be determined as follows.

First, suppose the desired signal arrives from angle θ_d relative to broadside. (θ is defined in Figure 1.) Let $\tilde{d}(t)$ be the desired signal waveform as received on element 1. Then the desired signal at an arbitrary tap is

$$\tilde{d}_{mk}(t) = \tilde{d}(t-[k-1]T_o-[m-1]T_d), \tag{11}$$

where T_o is the delay between taps and T_d is the desired signal spatial propagation delay between adjacent elements,

$$T_d = \frac{L}{c} \sin\theta_d, \tag{12}$$

with L the element separation (see Figure 1) and c the velocity of propagation. We assume $\tilde{d}(t)$ is a zero-mean, stationary, random process with average power p_d,

$$p_d = E[\,|\tilde{d}(t)|^2\,] \ . \tag{13}$$

The signal $\tilde{d}_o(t)$ in (7) is identical to $\tilde{d}(t)$ except normalized to have unit power,

$$\tilde{d}_o(t) = \frac{1}{\sqrt{p_d}} \tilde{d}(t) \ . \tag{14}$$

Next, assume the interference arrives from angle θ_i and has waveform $\tilde{i}(t)$ at element 1. The interference signal at an arbitrary tap is then

$$\tilde{i}_{mk}(t) = \tilde{i}(t-[k-1]T_o-[m-1]T_d), \tag{15}$$

where T_i is the interference propagation delay between elements,

$$T_i = \frac{L}{c}\sin\theta_i \ . \tag{16}$$

We assume $\tilde{i}(t)$ is also a zero-mean stationary random process, statistically independent of $\tilde{d}(t)$.

Finally, assume each element signal contains a zero-mean thermal noise voltage $\tilde{n}_{m1}(t)$ of power σ^2, statistically independent between elements. Thus,

$$E[\tilde{n}_{m1}^{*}(t)\tilde{n}_{n1}(t)] = \sigma^2\delta_{mn}, \qquad 1\leq m,n\leq M, \tag{17}$$

where δ_{mn} is the Kronecker delta. The noise signal at an arbitrary tap is just a delayed version of the noise on that element,

$$\tilde{n}_{mk}(t) = \tilde{n}_{m1}(t-[k-1]T_o) \ . \tag{18}$$

The $\tilde{n}_{m1}(t)$ are assumed independent of $\tilde{d}(t)$ and $\tilde{i}(t)$.

With these definitions, we may determine Φ and S in (6,7). Because the desired, interference and thermal noise terms are all mutually independent and zero-mean, Φ splits into desired, interference, and thermal noise terms,

$$\Phi = \Phi_d + \Phi_i + \Phi_n \ . \tag{19}$$

Consider Φ_d first. In partitioned form, Φ_d is

$$\Phi_d = \begin{bmatrix} \Phi_{d11} & \Phi_{d12} & \cdots & \Phi_{d1M} \\ \Phi_{d21} & \Phi_{d22} & & \\ \vdots & & \ddots & \\ \Phi_{dM1} & & & \Phi_{dMM} \end{bmatrix} , \tag{20}$$

where each K x K submatrix Φ_{dmn} is the desired signal covariance matrix associated with a pair of element signal vectors X_{dm} and X_{dn},

$$\Phi_{dmn} = E[X_{dm}^{*} X_{dn}^{T}] . \tag{21}$$

Φ_{dmn} may be found by substituting $\tilde{d}_{mk}(t)$ of (11) into (21). The jk^{th} term of Φ_{dmn} (the element in the j^{th} row and k^{th} column of Φ_{dmn}) is found to be

$$[\Phi_{dmn}]_{jk} = R_d[(j-k)T_o + (m-n)T_d] , \tag{22}$$

where $R_d(\tau)$ is the autocorrelation function of the desired signal $\tilde{d}(t)$,

$$R_d(\tau) = E[\tilde{d}^{*}(t)d(t+\tau)] . \tag{23}$$

To have a specific case to use for calculations below, we shall assume $\tilde{d}(t)$ has a flat, bandlimited power spectral density $S_d(\omega)$ equal to $\frac{2\pi p_d}{\Delta\omega_d}$ over a bandwidth $\Delta\omega_d$ centered at carrier frequency ω_o, as shown in Figure 2(a). $R_d(\tau)$ is then the inverse Fourier Transform of $S_d(\omega)$, or

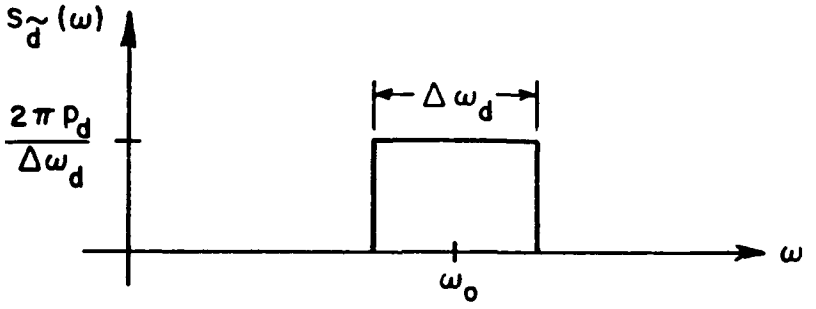

(a) THE DESIRED SIGNAL POWER SPECTRAL DENSITY

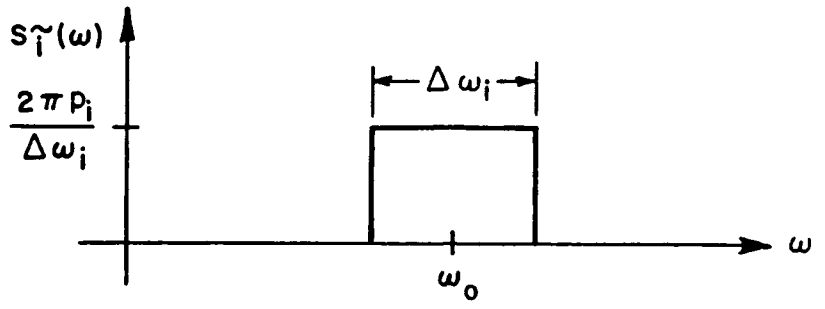

(b) THE INTERFERENCE POWER SPECTRAL DENSITY

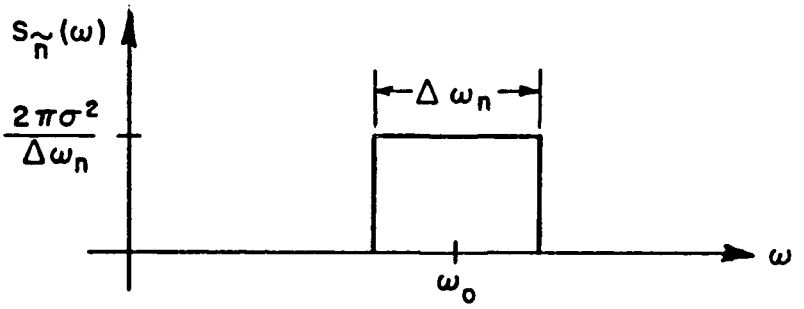

(c) THE THERMAL NOISE SPECTRAL DENSITY

Figure 2. The Assumed Spectral Densities.

$$R_d(\tau) = p_d \, \mathrm{sinc}\left(\frac{\Delta\omega_d \tau}{2}\right) e^{j\omega_o \tau} \quad . \tag{24}$$

p_d is the desired signal power received per array element, as defined in (13), and sinc(x) denotes sin(x)/x.

For a specific arrival angle θ_d and tap delay T_o, the matrix Φ_d in (20) can be determined by substituting (24) into (22). Before doing that, it is helpful to write the autocorrelation function in (22) in normalized form. From (24), we have

$$R_d[(j-k)T_o+(m-n)T_d] = p_d \mathrm{sinc}\left\{\frac{\Delta\omega_d}{2}[(j-k)T_o+(m-n)T_d]\right\} e^{j\omega_o[(j-k)T_o+(m-n)T_d]} \quad . \tag{25}$$

Note first that the product $\Delta\omega_d T_d$ may be written

$$\Delta\omega_d T_d = \frac{\Delta\omega_d}{\omega_o}(\omega_o T_d) = B_d \phi_d, \tag{26}$$

where B_d is the desired signal relative bandwidth,

$$B_d = \frac{\Delta\omega_d}{\omega_o} \, , \tag{27}$$

and ϕ_d is the interelement phase shift at the carrier frequency ω_o,

$$\phi_d = \omega_o T_d = \pi \sin\theta_d \, . \tag{28}$$

In addition, it is helpful to write T_o, the time delay between taps, in normalized form. Because earlier papers have often assumed a quarter wavelength delay between taps [2], we shall arbitrarily normalize T_o to the time associated with a quarter wavelength delay. The time delay required to produce a 90° shift at frequency ω_o is

$$T_{90°} = \frac{\pi}{2\omega_o} \cdot \tag{29}$$

Therefore we write T_o in the form

$$T_o = rT_{90°} = \frac{\pi r}{2\omega_o} \cdot \tag{30}$$

r is the number of quarter-wave delays in T_o at frequency ω_o. Then we also have

$$\Delta\omega_d T_o = \Delta\omega_d \frac{\pi r}{2\omega_o} = \frac{\pi}{2} rB_d \cdot \tag{31}$$

In terms of the normalized parameters B_d, ϕ_d and r, the jk^{th} element of Φ_{dmn} is

$$[\Phi_{dmn}]jk = p_d \operatorname{sinc}\left[\frac{Bd}{2}\left[\frac{\pi}{2}(j-k)r+(m-n)\phi_d\right]\right] e^{j[\pi/2(j-k)r+(m-n)\phi_d]} \cdot \tag{32}$$

The interference matrix Φ_i in (19) may be found in the same way. Φ_i is

$$\Phi_i = \begin{bmatrix} \Phi_{i11} & \Phi_{i12} & \cdots & \Phi_{i1M} \\ \Phi_{i21} & \Phi_{i22} & \cdots & \\ \vdots & \vdots & \ddots & \\ \Phi_{iM1} & & & \Phi_{iMM} \end{bmatrix}, \tag{33}$$

where each K x K submatrix Φ_{imn} is the covariance matrix for the element signal vectors X_{im} and X_{in},

$$\Phi_{imn} = E[X_{im}^{*} X_{in}^{T}] \quad . \tag{34}$$

The jk^{th} element of Φ_{imn} is

$$[\Phi_{imn}]_{jk} = R_i[(j-k)T_o+(m-n)T_i] \quad , \tag{35}$$

where $R_i(\tau)$ is the autocorrelation function of the interference,

$$R_i(\tau) = E[\tilde{i}^{*}(\tau)\tilde{i}(t+\tau)] \quad . \tag{36}$$

We shall assume the interference also has a flat, bandlimited power spectral density $S_i(\omega)$ equal to $\frac{2\pi p_i}{\Delta\omega_i}$ over bandwidth $\Delta\omega_i$, as shown in Figure 2(b). p_i is the interference power received per element. $R_i(\tau)$ is then

$$R_i(\tau) = p_i \ \text{sinc}\left(\frac{\Delta\omega_i\tau}{2}\right)e^{j\omega_o\tau} \quad . \tag{37}$$

Substituting T_o and T_i in (35) and normalizing as in (32) gives

$$[\Phi_{imn}]_{jk} = p_i \text{sinc}\left\{\frac{B_i}{2}\left[\frac{\pi}{2}(j-k)r+(m-n)\phi_i\right]\right\}e^{j[\pi/2(j-k)r+(m-n)\phi_i]} \quad , \tag{38}$$

where B_i is the relative bandwidth of the interference,

$$B_i = \frac{\Delta\omega_i}{\omega_o}, \tag{39}$$

and ϕ_i is the interelement phase shift for the interference at carrier frequency ω_o,

$$\phi_i = \omega_o T_i = \pi \sin\theta_i \ . \tag{40}$$

The noise matrix Φ_n in (19) is slightly different because the noise is independent between elements, so the noise cross-products are zero except for those associated with the same element. We have

$$\Phi_i = \begin{bmatrix} \Phi_{n11} & 0 & & 0 \\ 0 & \Phi_{n22} & & \\ & & \ddots & \\ 0 & & & \Phi_{nMM} \end{bmatrix} . \tag{41}$$

We assume the noise power spectral density $S_n(\omega)$ is equal to $\frac{2\pi\sigma^2}{\Delta\omega_n}$ over a bandwidth $\Delta\omega_n$, as shown in Figure 2(c). The jk^{th} element of Φ_{nmm} is then

$$[\Phi_{nmm}]_{jk} = \sigma^2 \text{sinc}\left[\frac{B_n}{4}(j-k)r\pi\right] e^{\pi/2(j-k)r} \ , \tag{42}$$

where B_n is the relative noise bandwidth,

$$B_n = \frac{\Delta\omega_n}{\omega_o} \ . \tag{43}$$

We have now obtained all terms in the matrix Φ of (6).

Next, consider the steering vector S of (7). Because the interference and noise vectors X_i and X_n are independent of $\tilde{d}(t)$, the only term that contributes to (7) is X_d:

$$S = E[X^* \tilde{d}_o(t)] = E[X_d^* \tilde{d}_o(t)] \quad . \tag{44}$$

Substituting for X_d and using (14) gives

$$S = \begin{bmatrix} s_{11} \\ s_{12} \\ \vdots \\ s_{1k} \\ s_{21} \\ s_{22} \\ \vdots \\ s_{2k} \\ \vdots \\ s_{M1} \\ \vdots \\ s_{Mk} \end{bmatrix} \begin{matrix} \\ \\ \\ \\ \\ \\ \\ \\ \\ \\ \\ \\ \end{matrix} \begin{matrix} \text{Element 1} \\ \\ \\ \\ \text{Element 2} \\ \\ \\ \\ \\ \text{Element M} \\ \\ \\ \end{matrix} , \tag{45}$$

where

$$s_{mk} = \sqrt{p_d}\ \text{sinc}\ \{\frac{B_d}{2}[\frac{\pi}{2}(j-1)r+(m-1)\phi_d]\} e^{j[\pi/2(j-1)r+(m-1)\phi_d]} \quad . \tag{46}$$

From Φ and S, the optimal array weight vector may be computed from (5).

In solving (5), it is helpful to make one more normalization. Every element of the matrix Φ_d contains the constant p_d, every element of Φ_j contains p_j, and every element of Φ_n contains σ^2. If we divide the entire set of equations by σ^2, the solution for W will then depend on the normalized parameters

$$\xi_d = \frac{P_d}{\sigma^2} = \text{desired signal-to-noise ratio (SNR) per element,} \quad (47)$$

and

$$\xi_i = \frac{P_i}{\sigma^2} = \text{interference-to-noise ratio (INR) per element.} \quad (48)$$

From the optimal weight vector, we may compute the SINR (desired signal-to-interference-plus-noise ratio) at the array output. For a given W, the array output signal $\tilde{s}(t)$ is

$$\tilde{s}(t) = W^T X \ , \quad (49)$$

where X is the signal vector in (3). By writing X as in (10), we may split $\tilde{s}(t)$ into its desired, interference and noise components,

$$\tilde{s}(t) = \tilde{s}_d(t) + \tilde{s}_i(t) + \tilde{s}_n(t) \ , \quad (50)$$

where

$$\tilde{s}_d(t) = W^T X_d \ , \quad (51)$$

$$\tilde{s}_i(t) = W^T X_i \ , \quad (52)$$

and

$$\tilde{s}_n(t) = W^T X_n \ . \quad (53)$$

The output desired signal power is then

$$P_d = \frac{1}{2} E[\tilde{s}_d^*(t)\tilde{s}_d(t)]$$

$$= \frac{1}{2} E[W^\dagger X_d^* X_d^T W] = \frac{1}{2} W^\dagger \Phi_d W \ , \quad (54)$$

where † denotes the conjugate transpose. Similarly, the output interference and thermal noise powers are

$$P_i = \frac{1}{2} W^{\dagger} \Phi_i W \ , \tag{55}$$

and

$$P_n = \frac{1}{2} W^{\dagger} \Phi_n W \ . \tag{56}$$

Finally, the output SINR is

$$\text{SINR} = \frac{P_d}{P_i + P_n} \ . \tag{57}$$

In the next section, we apply these equations to a two-element array.

III. THE PERFORMANCE OF A TWO-ELEMENT ARRAY

Now let us consider the bandwidth performance of a simple two-element array with tapped delay-lines and see how this performance depends on the delay-line parameters.

First, for later comparison, we show in Figure 3 the SINR of a two-element array with a single complex weight (and no delay) behind each element. In this figure, the desired signal arrives from broadside (θ_d=0°) and the interference from an arbitrary angle θ_i. The SINR is plotted as a function of θ_i. The desired, interference and noise signals are all assumed to have the same bandwidth B, and Figure 3 shows the SINR for B=0, 0.01, 0.02, 0.05 and 0.2. ξ_d (the SNR per element) is 0 dB and ξ_i (the INR per element) is 40 dB for all curves.

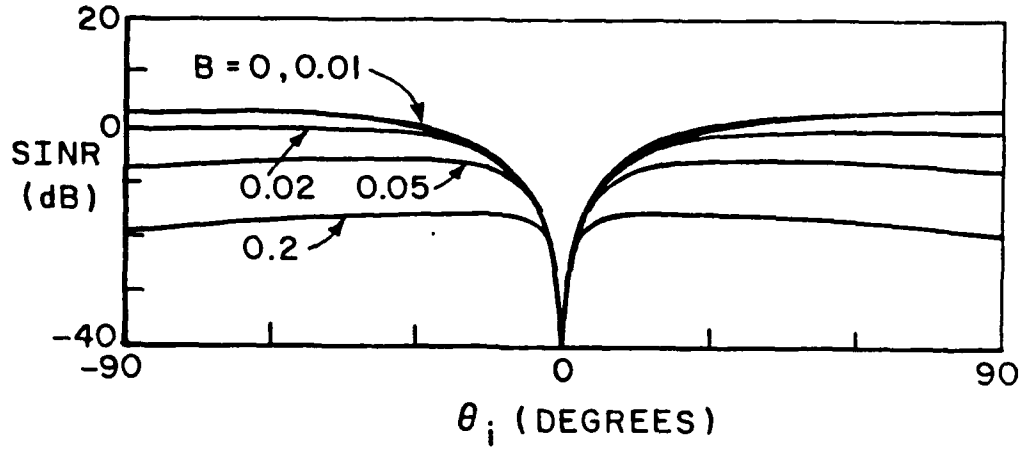

Figure 3. SINR vs. θ_j.
M=2, K=1
θ_d=0°, ξ_d=0 dB, ξ_j=40 dB

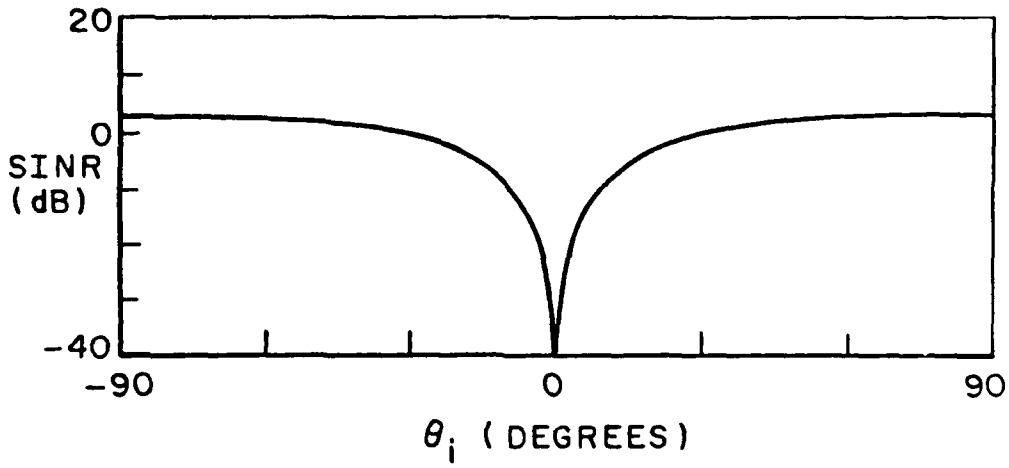

Figure 4. SINR vs. θ_j.
M=2, K=2, B=0.2
θ_d=0°, ξ_d=0 dB, ξ_j=40 dB

Figure 3 shows that when B = 0.01 the output SINR has dropped about 1 dB below its value with CW (zero bandwidth) signals. Larger bandwidths quickly reduce the SINR. For B=0.2, the largest value we show, there is as much as 22 dB degradation for some θ_i[1]. For such large bandwidths, the array performance is clearly unsuitable.

Now suppose we add a single quarter wavelength delay and one extra weight behind each element. (In the equations of Section II, we let K=2 and r=1.) Figure 4 shows the output SINR that results for this case with B=0.2 and with all other parameters the same as in Figure 3. We see that the array now performs essentially as well as the simple array in Figure 3 with CW signals. Thus, adding a single extra tap to each element, with a quarter wavelength between taps, has fully overcome the bandwidth degradation.

Figures 3 and 4 were computed for θ_d=0°. However, the results are similar for other values of θ_d. In general, when the array has a single weight behind each element, the SINR for B=0.2 is much poorer than for B=0. But if a single quarter wave delay and one extra tap are added to each element, the performance is fully restored.

Now consider what happens if we change the amount of delay between taps. The curves in Figure 4 were computed for a one-quarter wavelength delay between taps (r=1), an arbitrary amount. When other values of r are used, one finds a surprising result: the array output SINR is

---

[1] In general, the amount of degradation for a given bandwidth is strongly influenced by the INR. The larger the INR, the more sensitive the array is to interference bandwidth. In this discussion, we shall simple present results for an INR of 40 dB.

hardly affected by r! On the one hand, if r is reduced below 1, even to an artibtarily small value, the SINR is not noticeably different from that for r=1. A plot of SINR vs. θ_j for $r=10^{-4}$, for example, looks identical to Figure 4. On the other hand, if r is raised above 1, there is also very little change in SINR, until the delay exceeds about two wavelengths. For example, Figure 5 shows the SINR versus θ_j for r=5, 10, 15, 20 and 25 and for all other parameters the same as in Figure 4. Note that when r=5 the SINR still achieves the optimal value shown in Figure 4. When r=10 the SINR has dropped about 1 dB below optimal. (r=10 corresponds to 2.5 wavelengths of delay between taps.) For r=15 and above, the degradation is more serious, particularly for θ_j near $\pm 90°$.

Thus, the array performance is rather insensitive to r. Any value of r in the range $0<r<5$ yields essentially the same SINR. At first glance, this result seems puzzling, especially the fact that the SINR is unaffected when r approaches zero. Intuitively, it appears that a tapped delay line should become equivalent to a single weight when the delay is very small. However, this is not the case, as we shall see below.

To understand the effect of r on the array performance, we consider the transfer function of the array as seen by the interference. Let $H_m(\omega)$ be the transfer function of the delay line behind element m in Figure 1. In general, with K taps and K-1 delays behind m, $H_m(\omega)$ is

$$H_m(\omega) = w_{m1} + w_{m2} e^{-j\omega T_o} + \text{---} + w_{mk} e^{-j\omega(k-1)T_o} . \qquad (58)$$

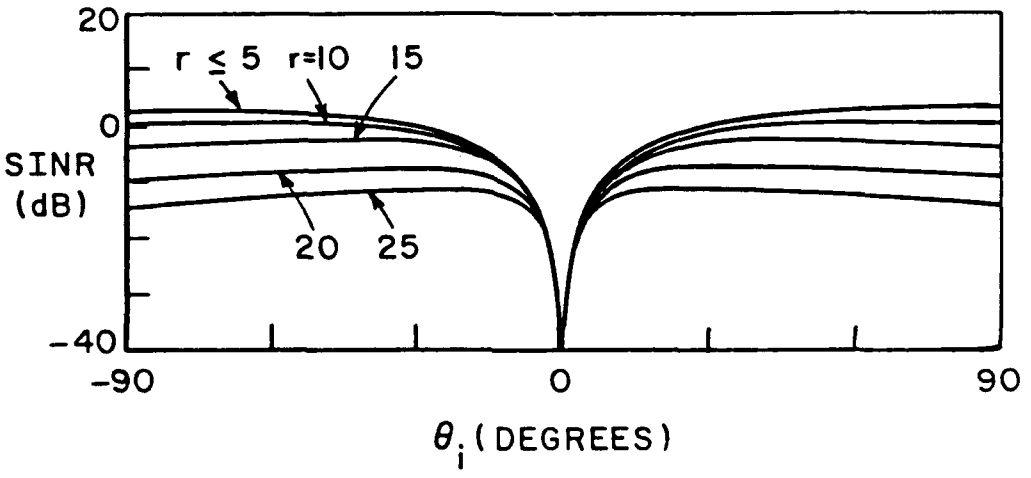

Figure 5. SINR vs. θ_j.
M=2, K=2, B=0.2
θ_d=0°, ξ_d=0 dB, ξ_i=40 dB

The transfer function of the entire array as seen by the interference, $H_i(\omega)$, is then

$$H_i(\omega) = \sum_{m=1}^{M} H_m(\omega) e^{-j\omega(m-1)T_i} , \tag{59}$$

where T_i is given in (16). To null an interference signal completely, $H_i(\omega)$ must be zero over the interference bandwidth. For the special case of a two-element array, as considered in Figures 3 and 4, $H_i(\omega)$ will be zero if

$$H_1(\omega) = -H_2(\omega) e^{-j\omega T_i} . \tag{60}$$

The physical meaning of (60) is easy to see. An interference signal from angle θ_i arrives at element 2 a time T_i later than at element 1. When the interference has nonzero bandwidth, this delay reduces the correlation between the signals on the two elements and makes it more difficult to null the interference by subtracting one element signal from another. However, if the filters $H_1(\omega)$ and $H_2(\omega)$ satisfy (60), the factor $e^{-j\omega T_i}$ in (60) will delay the interference an additional time T_i in element 1 to restore its correlation with the interference on element 2. The minus sign in (60) will then make the interference cancel at the array output.

Before considering what happens as r is varied, let us see how well (60) is satisfied by the arrays considered in Figures 3-5. Note that to satisfy (60), the transfer functions $H_1(\omega)$ and $H_2(\omega)$ must have identical amplitudes,

$$|H_1(\omega)| = |H_2(\omega)| \ , \tag{61}$$

and phases whose difference varies linearly with frequency,

$$\angle H_1(\omega) = \angle H_2(\omega) = \pi - \omega T_i \ , \tag{62}$$

over the signal bandwidth. For the array in Figure 3, we assumed one weight and no delays behind each element. For this case each $H_m(\omega)$ is simply

$$H_m(\omega) = w_{m1} \ , \tag{63}$$

which is a constant independent of frequency. With such an $H_m(\omega)$, it is possible to satisfy (60) at one frequency, but not over a band of frequencies. For the array in Figure 4, however, we assumed two weights and one delay behind each element. In this case each $H_m(\omega)$ has the form

$$H_m(\omega) = w_{m1} + w_{m2} e^{-j\omega T_o} \ . \tag{64}$$

Because of the term $e^{-j\omega T_o}$, the $H_m(\omega)$ can now vary with frequency. This capability allows $H_1(\omega)$ and $H_2(\omega)$ to do a better job of satisfying (60) over the signal bandwidth and hence improves the array bandwidth performance, as Figure 4 shows.

Examination of the $H_1(\omega)$ and $H_2(\omega)$ that actually result when each element has two weights and one delay confirm that the processor does attempt to satisfy (60). For example, Figure 6 shows $|H_1(\omega)/H_2(\omega)|$ and $\angle H_1(\omega) - \angle H_2(\omega)$ vs. ω for the same parameters as in Figure 4: $\theta_d = 0°$,

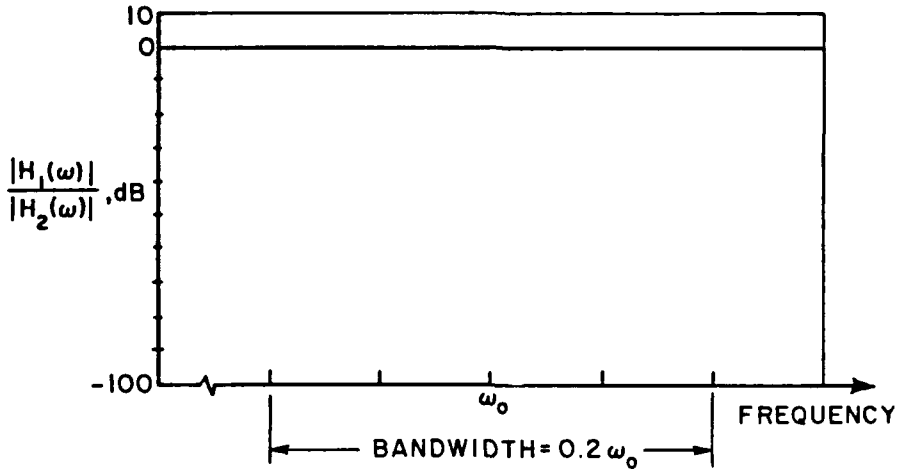

(a) $\frac{|H_1(\omega)|}{|H_2(\omega)|}$ vs. ω

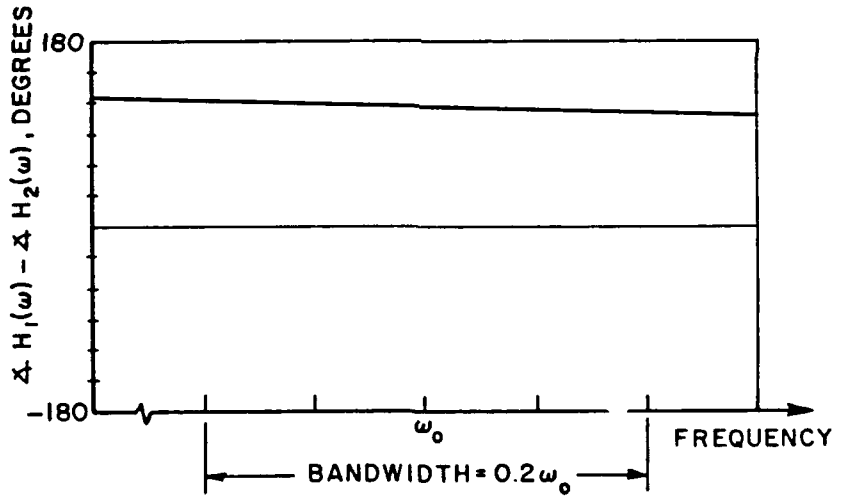

(b) $\measuredangle H_1(\omega) - \measuredangle H_2(\omega)$ vs. ω

Figure 6. The Transfer Functions $H_1(\omega)$ and $H_2(\omega)$.
M=2, K=2, B=0.2
θ_d=0°, θ_i=20°, ξ_d=0 dB, ξ_i=40 dB

ξ_d=0 dB, ξ_i=40 dB, r=1 and B=0.2, and for θ_i=20°. It may be seen how $|H_1(\omega)/H_2(\omega)|$=0 dB and $\angle H_1(\omega)-\angle H_2(\omega)$ varies linearly with frequency over the signal bandwidth. The slope of $\angle H_1(\omega)-\angle H_2(\omega)$ has the proper value to satisfy (60).

Now consider how the delay between taps affects the performance. First, suppose we let r approach zero. For very small r (small T_o), $H_m(\omega)$ in (64) becomes

$$H_m(\omega) = w_{m1} + w_{m2}\cos\omega T_o - jw_{m2}\sin\omega T_o$$

$$\cong w_{m1} + w_{m2} - jw_{m2}\omega T_o \ . \qquad (65)$$

We observe that no matter how small T_o is (as long as $T_o \neq 0$), the array can always realize any given linear slope for $\angle H_1(\omega)-\angle H_2(\omega)$ by making the weights sufficiently large. Calculations show that that is what happens. As r is reduced toward zero, the weights obtained from (5) increase without bound. Figure 7 illustrates this behavior. It shows $Re(w_{11})$ and $Im(w_{11})$ as functions of r for θ_d=0°, θ_i=20°, ξ_d=0 dB, ξ_i=40 dB, and B=0.2, the same parameters as above. The other weights behave similarly as $r \to 0$.

Thus, by increasing the weights, the array can satisfy (60) regardless of how small r becomes (as long as $r \neq 0$). This is the reason an array with two weights and one delay behind each element does not become equivalent to an array with a single weight behind each element as $r \to 0$. With two weights and one delay, the SINR obtained vs. θ_i does not change significantly from that in Figure 4 as $r \to 0$.

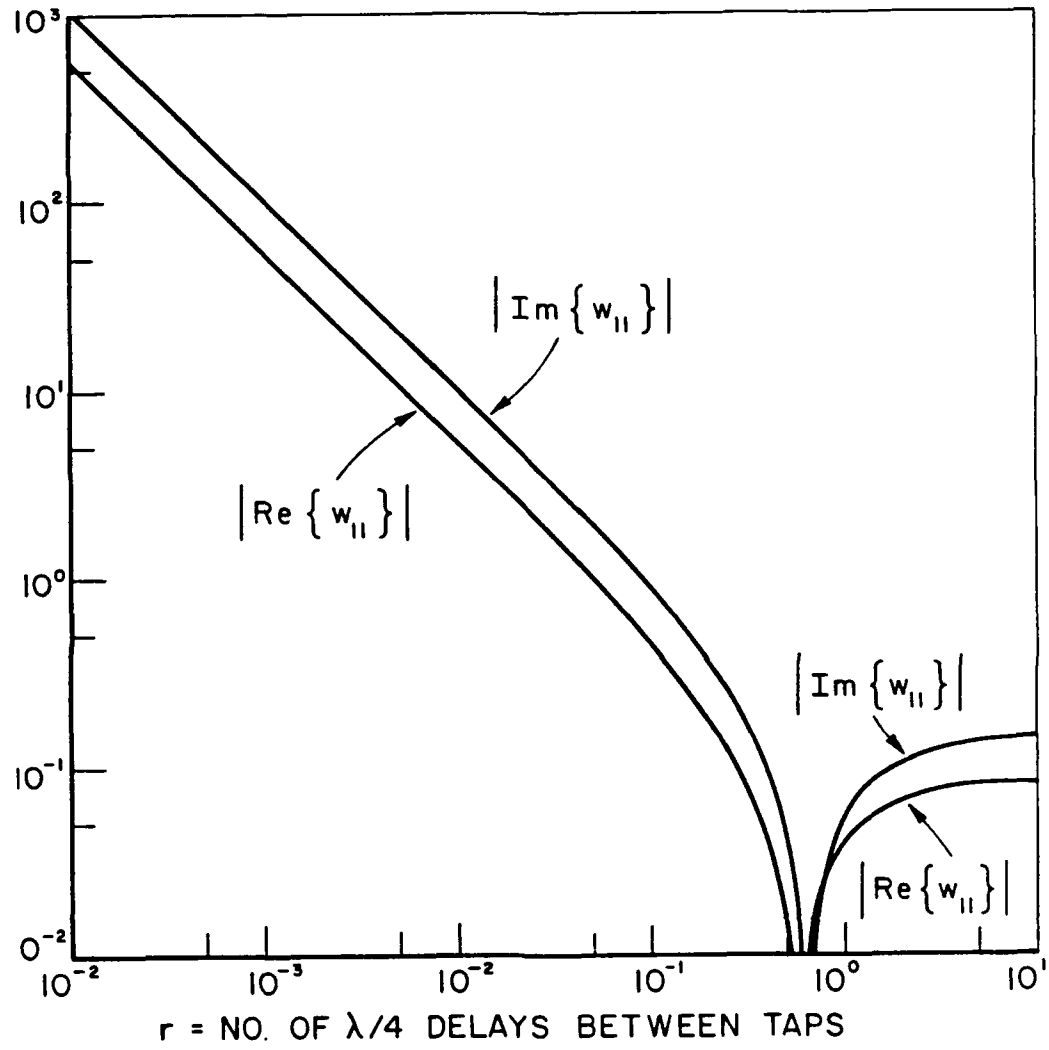

Figure 7. w_{11} versus r.
θ_d=0°, θ_i=20°, ξ_d=0 dB,
ξ_i=40 dB, B=0.2.

The unbounded increase in the weights as $r \to 0$ is understandable if we also note that the covariance matrix in (6) becomes singular when r goes to zero. As $r \to 0$, the signal $\tilde{x}_{m2}(t)$ at the second tap becomes equal to $\tilde{x}_{m1}(t)$, the signal at the first tap. In the limit, when two tap signals are equal, the covariance matrix in (6) will have two identical columns (or rows) and hence will be singular. Thus we should expect the weight vector W satisfying (5) to exhibit unusual behavior as $r \to 0$.

In a hardware array, there is always a limit to how large the weights can actually become, of course. With analog weights, the circuits always saturate at some point. With digital weights, finite register lengths limit the maximum attainable weight values. Because the weights cannot increase indefinitely in a real array, there will be some minimum value of r for which the array can maintain the SINR. Below this minimum r, the SINR will drop.

Now consider what happens if we increase r. We showed in Figure 5 that when r is increased, the array performance is unaffected at first. But finally, for large values of r, the performance begins to drop. The explanation for this behavior may again be found by considering the $H_m(\omega)$.

For any value of r, nulling the interference requires the transfer functions $H_1(\omega)$ and $H_2(\omega)$ in a two-element array to satisfy (60) over the interference bandwidth. However, note that $H_m(\omega)$ in (58) is a periodic function of frequency. (It is a finite Fourier Series.) The period of $H_m(\omega)$ is

$$\Omega_0 = \frac{2\pi}{T_0} = \frac{4\omega_0}{r} . \tag{66}$$

For small r, this period is much larger than the signal bandwidth. But when r is increased, the period drops. Ω_0 will equal the signal bandwidth when

$$r = \frac{4}{B} . \tag{67}$$

When r is small and the period is much larger than the bandwidth, $\angle H_1(\omega)-\angle H_2(\omega)$ can easily approximate a linear function of frequency over the signal bandwidth (as seen for example in Figure 6). But if r is large enough, the period Ω_0 becomes comparable to the signal bandwidth. Because the $H_m(\omega)$ are periodic, it then becomes difficult for the $H_m(\omega)$ to satisfy (60) over the whole bandwidth. In particular, when $r>4/B$, $\angle H_1(\omega)-\angle H_2(\omega)$ cannot vary linearly over the entire bandwidth, since its value must repeat periodically within the bandwidth. This is the reason array performance drops when r becomes too large.

Figure 5, computed for B=0.2, illustrates this point. For B=0.2, the period Ω_0 will equal the signal bandwidth when r=20. One finds that there is no drop in SINR for r up to about 5 (which is 1/B). Beyond 5, the SINR drops as r approaches and then passes 20. We find the same general result for all values of B (up to B=0.5): <u>when the array has two weights and one delay behind each element, the SINR is unaffected by r as long as r is in the range $0<r<1/B$</u>.

The performance degradation for large r may also be understood from a time domain point of view. Signals with nonzero bandwidth remain

correlated with themselves for time shifts up to approximately the reciprocal of the bandwidth. Hence, one would expect that adding an extra delay and tap to each element will be effective only if the delays are short compared with the reciprocal of the bandwidth. If the delays are too large, the signals on different taps become decorrelated, and the array cannot null the interference by subtracting one tap signal from another.

The curves in Figures 4 and 5 assumed two weights and one delay behind each element. Let us now consider what happens if we add extra taps (extra delays and weights) behind each element in two-element array.

We observe first that adding extra taps can help the performance only for a limited range of r. On the one hand, when $r<1/B$, the array is already capable of nulling a wideband interference signal. Hence for $r<1/B$ there appears to be no point in adding extra taps. On the other hand, if $r>4/B$, the period Ω_0 of the $H_m(\omega)$ is less than the signal bandwidth. In this case the $H_m(\omega)$ cannot satisfy (60) over the signal bandwidth, regardless of how many taps are used, because $\angle H_1(\omega)-\angle H_2(\omega)$ must repeat periodically within the signal bandwidth. Hence the only case where extra taps may be useful is when $1/B<r<4/B$. In this range, the period of $H_m(\omega)$, although larger than the bandwidth, is small enough that with only two weights and one delay $\angle H_1(\omega)-\angle H_2(\omega)$ does not vary linearly with frequency. However, adding more Fourier terms in (58) will allow $\angle H_1(\omega)-\angle H_2(\omega)$ to approximate a linear behavior more accurately.

Let us illustrate this behavior for B=0.2. First, for $r<(1/B)=5$, no extra taps are needed. An array with one delay and two weights already has optimal performance, as may be seen in Figure 4. Next, for $5<r<20$, we find that with only two weights and one delay, the SINR is reduced from that in Figure 4. Figure 5 shows this behavior. However, for this range of r, the performance will improve if we increase the number of taps. Figure 8 shows the SINR versus θ_i for r=15 and for K=2, 4, 8 and 16 taps. As may be seen, for this r the performance is improved by increasing K. The reason for this improvement is seen in Figure 9, which shows $\angle H_1(\omega)-\angle H_2(\omega)$ vs. ω for the same cases. $\angle H_1(\omega)-\angle H_2(\omega)$ becomes more nearly linear with ω over the signal bandwidth as K increases. ($|H_1(\omega)/H_2(\omega)|$ is unity over the bandwidth for all four values of K.)

Finally, when $r>(4/B)=20$, we expect poor nulling performance no matter how many extra taps are added, because $\angle H_1(\omega)-\angle H_2(\omega)$ is periodic with a period smaller than the bandwidth. Figure 10 shows such a case. It shows the SINR versus θ_i for r=22 (with B=0.2, $\theta_d=0°$, $\xi_d=0$ dB, $\xi_i=40$ dB) and for K=2, 4, 8 and 16. As may be seen, the SINR improves somewhat with K but never achieves the value in Figure 4. Figure 11 shows $|H_1(\omega)/H_2(\omega)|$ and $\angle H_1(\omega)-\angle H_2(\omega)$ for these same cases. Note how $|H_1(\omega)/H_2(\omega)|$ and $\angle H_1(\omega)-\angle H_2(\omega)$ repeat periodically within the signal bandwidth. Also, $|H_1(\omega)/H_2(\omega)|\neq 1$ at some frequencies within the bandwidth, and $\angle H_1(\omega)-\angle H_2(\omega)$ is not linear across the bandwidth, regardless of how many Fourier Series terms are used in the $H_m(\omega)$.

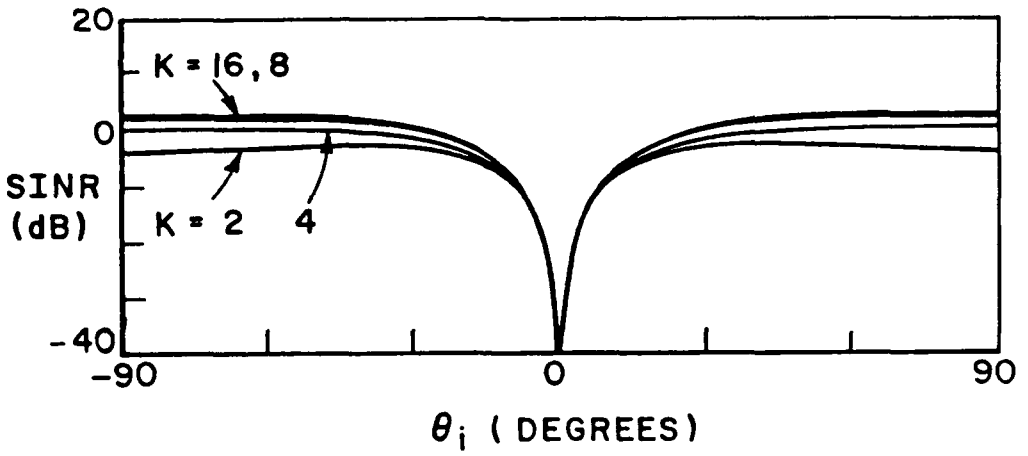

Figure 8. SINR vs. θ_i.
M=2, r=15, B=0.2
θ_d=0°, ξ_d=0 dB, ξ_i=40 dB

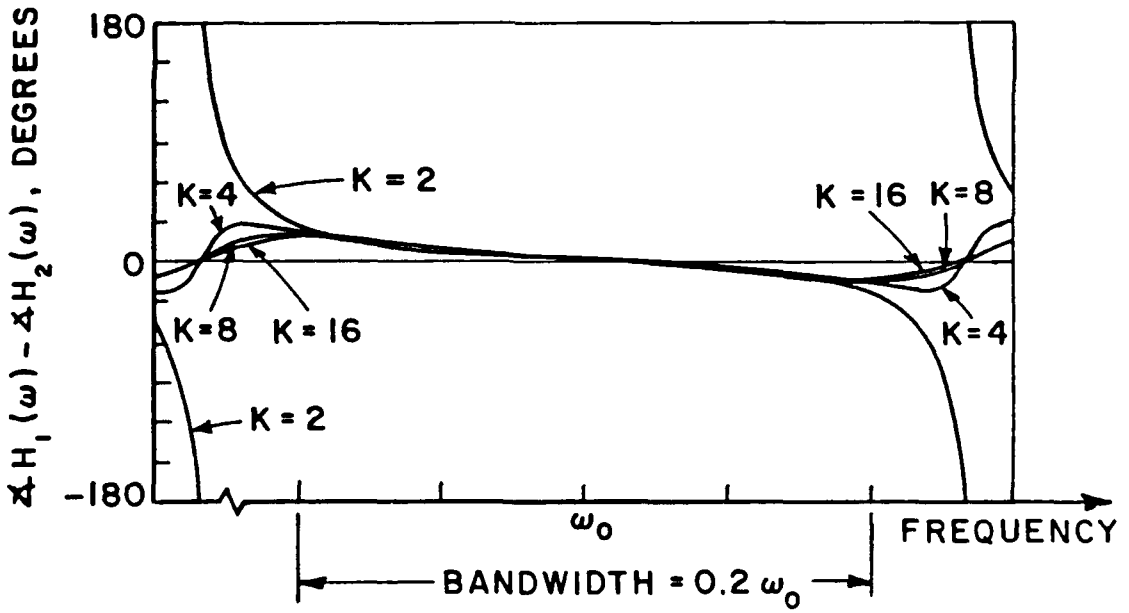

Figure 9. $\angle H_1(\omega) - \angle H_2(\omega)$ vs. ω.
M=2, r=15, B=0.2
θ_d=0°, ξ_d=0 dB, ξ_i=40 dB

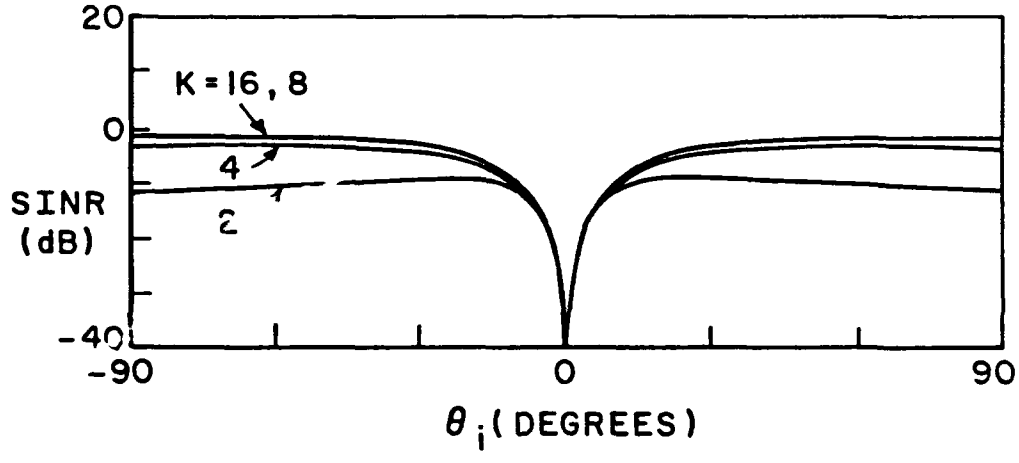

Figure 10. SINR vs. θ_i.
M=2, r=22, B=0.2
θ_d=0°, ξ_d=0 dB, ξ_i=40 dB

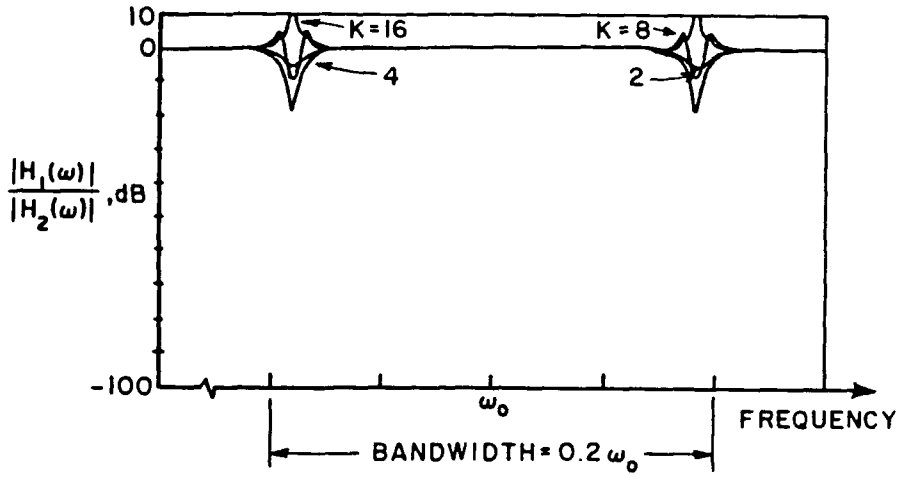

(a) $\frac{|H_1(\omega)|}{|H_2(\omega)|}$ vs. ω

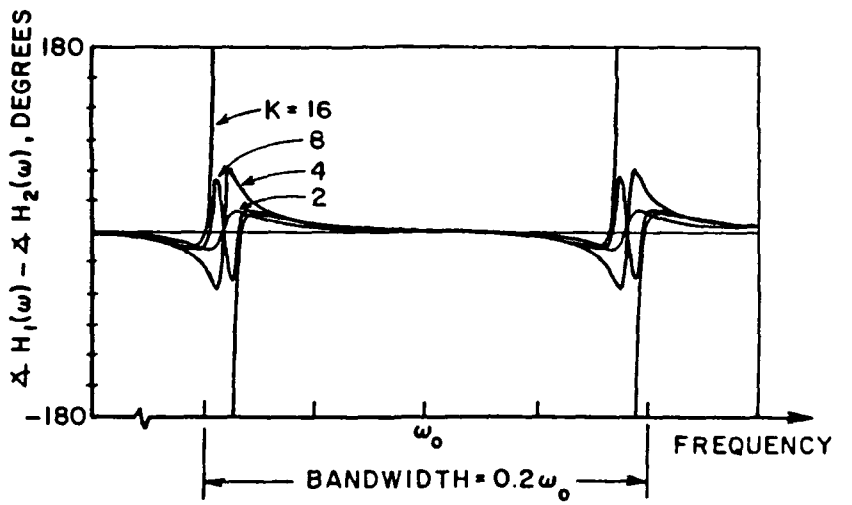

(b) $\measuredangle H_1(\omega) - \measuredangle H_2(\omega)$ vs. ω

Figure 11. The Transfer Functions $H_1(\omega)$ and $H_2(\omega)$.
M=2, r=22, β=0.2
θ_d=0°, ξ_i=0 dB, ξ_i=40 dB

Whether an adaptive array should be operated with r in the range $1/B<r<4/B$ and a large value of K depends on how the array is to be implemented. For an array with analog control loops, there is no reason to use such a large r. For one thing, it is difficult to implement long time delays between taps. For another, each weight in an adaptive processor adds complexity and cost to the processor. To obtain good bandwidth performance from the array, it is simpler just to use a small value of r, such as r=1, and to use only two weights and one delay per element.

For an array with digital weight control, on the other hand, an A/D converter will be used behind each element. In this case it may be useful to have a large value of r, since a large r corresponds to a low sampling rate. However, if r is large enough, more weights will be needed, as discussed above. The cost of increasing the number of weights depends on the algorithm used.[2]

Another factor that must be considered when r is large is the effect of the array on the desired signal. In general, an M-element array presents a transfer function

$$H_d(\omega) = \sum_{m=1}^{M} H_m(\omega) e^{-j\omega(m-1)T_d} \tag{68}$$

to the desired signal, where T_d is given in (12) and $H_m(\omega)$ in (58). If $H_d(\omega)$ has anything other than a constant amplitude and a linear phase

---

[2] For the discrete LMS algorithm [1], the computational burden increases linearly with the number of weights. For the Sample Matrix Inverse method [6], it increases with the cube of the number of weights.

slope over the desired signal bandwidth, the desired signal waveform will be distorted in passing through the array. Whether this is a problem or not depends on the desired signal waveform and the application. For many communication systems, however, it is difficult to accommodate a desired signal whose waveform changes as the array adapts.

Because the array responds to the incoming signals, $H_d(\omega)$ depends in general on all the signal parameters: the desired signal power and arrival angle and the interference power and arrival angle. However, for the two-element array considered above, the results show that when r is small ($r<1/B$), $|H_d(\omega)|$ is constant and $\angle H_d(\omega)$ varies linearly with frequency. But when $r>1/B$, $H_d(\omega)$ can vary substantially over the desired signal bandwidth. For r in the range $1/B<r<4/B$, one finds that $|H_d(\omega)|$ becomes more nearly constant and $\angle H_d(\omega)$ becomes more nearly linear with frequency as the number of weights K is increased. Figure 12 shows a typical case. It shows $|H_d(\omega)|$ and $\angle H_d(\omega)$ over the signal bandwidth for r=15 and k=2, 4, 8 and 16, with all other parameters the same as in Figures 8 and 9. Note how the behavior of $H_d(\omega)$ improves as K increases. On the other hand, for $4/B<r$, $H_d(\omega)$ cannot have the required behavior over the signal bandwidth, because the Fourier Series period is less than the signal bandwidth. In this case there is always at least some desired signal distortion, no matter how large K.

It is clear that a designer must take the behavior of $H_d(\omega)$ into account when a large value of r is used.

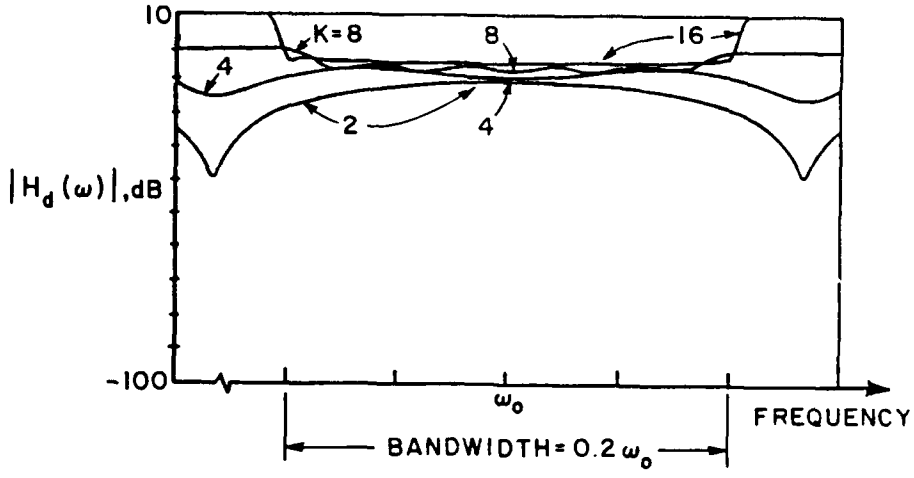

(a) $|H_d(\omega)|$ vs. ω.

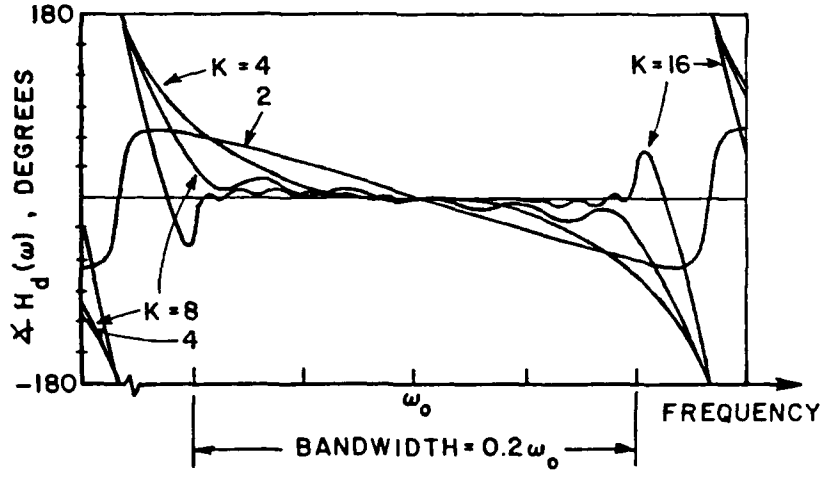

(b) $\angle H_d(\omega)$ vs. ω.

Figure 12. The Transfer Function $H_d(\omega)$.
M=2, r=15, B=0.2
θ_d=0°, ξ_d=0 dB, ξ_i=40 dB

IV. CONCLUSIONS

This report considered the bandwidth performance of a two-element adaptive array with tapped delay-lines behind the elements. Section II presented the equations used to compute the array output SINR (signal-to-interference-plus-noise ratio). Section III described how the number of taps and the delay between taps affects the SINR.

An array with two weights and one delay behind each element yields optimal performance (equal to that obtained with CW interference) for any value of delay greater than zero and less than T_{90}/B, where T_{90} is the time delay for a 90° carrier phase shift and B is the fractional signal bandwidth. Delays less than T_{90} yield optimal performance but result in large array weights. Delays larger than T_{90}/B yield suboptimal SINR when each element has only two weights.

For delays between T_{90}/B and $4T_{90}/B$, the performance is suboptimal with only two weights but approaches the optimal if more delay line sections and weights are added to each element. Delays larger than $4T_{90}/B$ result in suboptimal performance regardless of the number of delays and weights used.

REFERENCES

[1] B. Widrow, P.E. Mantey, L.J. Griffiths and B.B. Goode, "Adaptive Antenna Systems," Proc. IEEE, 55, 12 (December 1967), 2143.

[2] W.E. Rodgers and R.T. Compton, Jr., "Adaptive Array Bandwidth with Tapped Delay-Line Processing," IEEE Trans., AES-15, 1 (January 1979), 21.

[3] J.T. Mayhan, A.J. Simmins and W.C. Cummings, "Wideband Adaptive Antenna Nulling Using Tapped Delay Lines," IEEE Trans., AP-29, 6 (November 1981), 923.

[4] W.D. White, "Wideband Interference Cancellation in Adaptive Sidelobe Cancellers," IEEE Trans., AES-19, 6 (November 1983), 915.

[5] S.P. Applebaum, "Adaptive Arrays," IEEE Trans., AP-24, 5 (September 1976), 585.

[6] I.S. Reed, J.D. Mallett and L.E. Brennan, "Rapid Convergence Rate in Adaptive Arrays," IEEE Trans., AES-10, 6 (November 1974), 853.

[7] C.A. Baird, Jr., and C.L. Zahm, "Performance Criteria for Narrowband Array Processing," 1971 IEEE Conference on Decision and Control, Miami Beach, FL, December 15-17, 1971.